Synthesis and Characterization of Silver and Gold Nano-Structures on Chitosan-Porous Anodic Alumina Nano-Composite

Qayyum, Somia
Department of Chemistry, Mirpur University of Science and Technology (MUST), Mirpur, AJ&K-10250, PAKISTAN

Mehmood, Mazhar
Department of Metallurgy and Materials Engineering, Pakistan Institute of Engineering and Applied Sciences (PIEAS), Nilore, Islamabad-45650, PAKISTAN

Mirza, Muhammad A.*+
Department of Chemistry, Mirpur University of Science and Technology (MUST), Mirpur, AJ&K-10250, PAKISTAN

Ashraf, Sumaira
Department of Metallurgy and Materials Engineering, Pakistan Institute of Engineering and Applied Sciences (PIEAS), Nilore, Islamabad-45650, PAKISTAN

Ahmed, Zahoor
Department of Chemistry, Mirpur University of Science and Technology (MUST), Mirpur, AJ&K-10250, PAKISTAN

Tanvir, Tauseef
Department of Metallurgy and Materials Engineering, Pakistan Institute of Engineering and Applied Sciences (PIEAS), Nilore, Islamabad-45650, PAKISTAN

Choudhary, Muhammad A.; Iqbal, Massod; Nisar, Faria; Nisa, Zaib un
Department of Chemistry, Mirpur University of Science and Technology (MUST), Mirpur, AJ&K-10250, PAKISTAN

ABSTRACT: *This study was designed to probe the fabrication of unique silver and gold nano-structures engaging a self-designed chitosan-porous anodic alumina nano-composite as template. Porous anodic alumina have been manufactured by di-step aluminum anodization in oxalic acid electrolytic bath. The surface properties of porous anodic alumina were reinforced by chitosan neutralized in sodium hydroxide. Multifarious nano-morphologies of silver as well as gold nano-structures were observed. Furthermore, the long chitosan biopolymer chains were degraded by γ-irradiations and the same procedure was employed for modification of porous anodic alumina with γ-degraded chitosan. The morphologies of fabricated silver and gold*

***** *To whom correspondence should be addressed.*
+ E-mail: muhammadaslammirzachem@gmail.com
1021-9986/2019/6/31-44 *14/$/6.04*

nano-structures were investigated by scanning electron microscopy, while their composition was evaluated with the help of energy dispersive X-ray spectroscopy. X-ray diffraction study exposed face centered cubic phase for both silver and gold nano-structures. Reflection mode UV-Vis spectroscopy was used to ascertain reflection grooves in the absorption range of silver and gold nano-structures respectively. The technique does not involve any harmful reagent and show different selectivity than methods in general practice. The achieved results apprised that the fabricated nano-structures offer the advantages of biocompatibility and eco-friendliness for numerous biomedical uses.

KEYWORDS: *Porous anodic alumina; Di-step aluminum anodization; Chitosan; Nano-composite; Gold and silver nano-structures.*

INTRODUCTION

Recognition of Porous Anodic Alumina (PAA) as a scaffold material for fabrication of one-dimensional nano-materials started in early 1930's. Afterwards, it fired the research at nano-scale owing to its simple synthesis in a self-ordered frame of nano-channels. Anodization of aluminum gives a unique pattern of closely organized hexagonal cells with central holes. Cylindrical nano-pores having high facet ratio are formed by supervising key factors like nature and concentration of electrolyte, temperature and voltage throughout anodization and electro-polishing procedures. High optical, thermal and chemical stability, remarkable mechanical strength, self-organized uniform pores, tunable aspect ratio, no toxicological danger and affordability are the contributing gains of PAA, which decorate PAA in the nano-research domain [1-12]. Various Nano-Structures (NS) have been fabricated employing hexagonal nano-pores of PAA through molten metal injection, thermal decomposition of metallic salts [13], pulse electro-depositions [14], direct current and alternating current electro-deposition [15, 16], simple deposition [17, 18] etc. One-dimensional metal NS like nano-wires [19], nano-dots and nano-rods of various materials [20, 21] have been handily fabricated utilizing PAA template. PAA is a promising substitute to other commonly explored nano-porous platforms for the manufacture of self-assembled collection of metal NS. Gold (Au), Silver (Ag), Nickel (Ni) and Ag-Au nano-wires had been fabricated via electro-deposition technique [22, 23]. Sanjay et al. observed the comparative loading of silver nano-structures (Ag NS) on PAA substrate by employing different methods [24]. Hexagonal array of PAA have been utilized as reaction vessels for synthesis of isolated and highly ordered nano-crystals [25]. Mono-disperse Ag nano-wires have also been synthesized using PAA template [26, 27].

The nano-channel frame of PAA membrane is restricted to a tubular and flat pattern with uniform pore diameter. The development and modifications in anodization procedures promise the fabrication of more intricate PAA membranes with diverse geometries, desired functionalities and surface properties. These modifications mark PAA chemical/physical selective towards target molecules [28]. The specific surface properties and surface area of PAA can be strengthened by amending the hydroxyl rich surface with appropriate functionalities. Functionalized nano-porous membranes open up new opportunities for advance applications, especially for biomedical applications, in catalysis or as separators and filters. Functionalization of PAA can be achieved by both organic and inorganic materials including metals [29], oxides [30-34], DNAs [35], proteins [36, 37], diamond [38, 39], diamond-like carbon [29, 38, 40] and polymers [41-46]. Polymers possessing necessary functionalities can either be infiltrated or covalently attached to the surface of PAA template. Polymer-modified PAA portray fortified selectivity, stability, binding capacity and biocompatibility in contrast to un-modified PAA surface [18]. Subsequent functionalized PAA membranes can be employed either to fabricate other functional NS (like nano-rods, nano-particles, nano-tubes) or target the biomolecules.

The synthesis of polymer-supported metal NS is of considerable interest because polymers offer efficient stabilization as compared to the recognized ligands like sodium borohydride or sodium citrate. In recent times, polymers having amino (NH_2) group are widely used because only one constituent is responsible for the reduction and stabilization processes. Chitosan (CS), a co-polymer of β-(1-4 linked)-2-acetamido-2-deoxy-D-glucopyranose and 2-amino-2-deoxy-D-glucopyranose, is a naturally harvested chitin derivative. Chitin, a poly-β-(1-4 linked)-2-acetamido-2-deoxy-D-glucopyranose, is an amino functionalized, non-elastic polymer which is white in appearance. Cell walls of yeast, fungi and exoskeleton of crustaceans naturally contain chitin. CS is obtained by chitin deacetylation. The extent of deacetylation is controlled by the adapted synthesis procedure and nature of source [47-51]. High abundance, low cost, non-toxicity, bio-degradation, bio-compatibility and presence of metal anchoring functional (free hydroxyl and amino) groups are the sparkling features of CS usage [52-55]. Therefore, CS can be used as a reducing and also as a stabilizing agent for metal NS fabrication [56-58]. Heavy metal (Zn^{+2}, Cu^{+2}) contaminants have been effectively removed using CS-capped Au nano-particles [59]. *Bo et al.* employed poly (dimethyl siloxane) films modified with CS for gold nano-structures (Au NS) preparation [60]. Shi et al. synthesized CS-PAA membrane having uniform pores and porosity [18]. *Li et al.* synthesized Fe^0 nano-wires on PAA template modified with chitosan and employed them as an adsorption system for removal of heavy metal from water. The modified adsorbent depicted superior adsorption efficiency than when only CS or PAA was used [61]. Cu^{+2} capped CS-PAA membranes have been fabricated by activating the PAA membrane with 3-glycidoxypropyltrimethoxysilane followed by CS grafting. These membranes have been fruitfully employed to separate and purify hemoglobin from red cell lysate [62]. Nevertheless, some of these approaches reflect various shortcomings like tedious work-up method, prolong reaction times, harsh reaction environments and use of expensive and lethal chemicals. Hence, a safe and mild approach employing cheap and ecofriendly reagents is still required for such makeover.

A detailed literature survey disclosed that only a few studies have been done using PAA template in combination with CS for metal nano-particle fabrication. So far, no progress has been made to fabricate Ag and Au NS embedded in CS-PAA nano-composite template. Therefore, this study aims at exploring a new convenient approach for the fabrication of Ag and Au NS using PAA template modified by CS and γ-irradiated chitosan (γ-ICS) under normal atmospheric conditions. Also the modification technique is cheap, reliable and modifies the whole surface of the PAA membrane. In the reported procedure, chemical reduction of subsequent metal ions into zero valent nano-particles has been carried out under gentle environment utilizing chitosan as a stabilizing and reducing agent. The crystalline character and surface morphology of these NS have also been inquired. Energy Dispersive X-ray (EDX) spectroscopy and X-Ray Diffraction (XRD) results also ascertained the presence of Ag and Au NS on CS-PAA nano-composite template. This work validates the fabrication of crystalline Au and Ag NS with variable morphologies employing the cited scaffold.

EXPERIMENTAL SECTION

Chemicals and apparatus

During the entire study, oxalic acid, per-chloric acid, acetone (Riedel), phosphoric acid sodium hydroxide, ethanol, chromic acid (Merck), acetic acid, tetrachloroauric (III) acid (Sigma Aldrich), silver nitrate (Fisher chemicals) and aluminum sheet (99.99% purity, Sigma Aldrich) were used. All chemicals used throughout this work were of analytical grade. Di-distilled water (specific resistance 18.2 MΩ.cm) was used. Morphology of Ag and Au-NS was examined with FEI-Nova Nano SEM-430. The X-ray diffraction patterns were recorded on Bruker D-8 Discover HR-XRD using CuK_α radiation (λ=1.5406 °A). The statistical details were dispersed within array 2θ=10°-90° (0.02° step size). Perkin Elmer Lambda 950 Spectrophotometer (Spectralon as reference) was used to acquire UV-Vis-NIR diffuse reflectance spectra.

Synthesis and preparation of PAA

A sheet of 99.99% pure Al (0.5 mm thickness) was cut into 1 x 3 cm size and annealed for five days at 500 °C in common muffle furnace and then ultrasonically degreased in acetone for 20 min. Two electrode cell used for electro-polishing and anodization consists of aluminum as anode (working electrode) and graphite as cathode (counter electrode). Electro-polishing for 20 min

at 20 V and 1°C temperature was done in alcohol-perchloric acid (4:1 v/v) (60 mL ethanol and 15 mL perchloric acid) solution to reduce surface roughness of Al strip. The electro-polished Al strip was anodized (first-step) in oxalic acid (0.3 M) solution for 3 h at 50 V and 1°C temperature. Alumina film, after first-step anodization, displayed a haphazard arrangement of hexagonal pores. The wet chemical etching technique was used to strip away this film at 80°C in (0.2 M) chromic and (0.4 M) phosphoric acid mixture for 3 h. The hollow pattern, obtained from oxide etching, provides nucleation sites for hexagonal and regular pore array formation during second-step anodizing. The second-step anodization, carried under same parameters as cited for first-step anodization, resulted in a regular hexagonal collection of pores. A aqueous solution of oxalic acid (0.3 M) was used for pore widening at room temperature for 30 min. PAA of 100-400 µm through thickness was used to fabricate nano-composite [63].

Fabrication of Ag and Au nano-structures on CS-PAA nano-composite template

Customary methods were employed to obtain CS from crab's shells [50], having 75% deacetylation degree. CS is soluble in acidified water. Acetic acid (5%) was used to prepare CS solution. PAA template was immersed in saturated CS solution at room temperature for 24 h. Chitosan interacts with hydroxyl groups of PAA film ensuring a link between chitosan and PAA surface [72]. The polymer functionalized PAA template was dried and treated with sodium hydroxide (NaOH) solution. The polycationic CS was neutralized by the NaOH solution, which appeared as a hydrated gel-like precipitation [64]. Ag and Au NS were fabricated by submerging the CS-PAA nano-composite in 1 mM precursor ($AgNO_3$ or $HAuCl_4.3H_2O$) solution for 24 h. Schematic representation for metal NS fabrication on CS-PAA nano-composite is given in Fig. 1.

Fabrication of Ag and Au nano-structures on γ-ICS-PAA nano-composite template

Cobalt-60 γ-irradiator (Model JS-7900, IR-148, ATCOP) was used to irradiate CS at Pakistan Radiation Services Lahore. CS was exposed to various doses of gamma radiations stretching from 25 to 100 kGy (dose rate=1.02 kGy/h). The irradiation was performed in air environment [69]. γ- Radiations degraded the long biopolymer chains and lowered their molecular weights. *Tahtat et al.* [65], *Zainol et al.* [66] and *Baroudi et al.* [67] suggested that irradiation decreases the molecular weight through de polymerization approach with insignificant influence on the chemical characteristics like deacetylation extent, functional groups of chitosan biopolymer. The γ-radiation dosages are secure, environmental favorable and free from initiator residues/chemicals [68-71].The γ-ICS solution was prepared in 5% acetic acid. Ag or Au deposition on γ-ICS-PAA nano-composite followed the same quoted procedure as for the metal deposition on CS-PAA nano-composite. The experimental settings employed for the synthesis of metal nano-structures on CS and γ-ICS-PAA nano-composite are tabulated in Table 1.

RESULTS AND DISCUSSION

Silver-chitosan/porous anodic alumina nano-structures (Ag-CS/PAANS)

Fig. 2(a-c) shows the scanning electron microscopy (SEM) micrograph of PAA and Ag-NS appeared after modification with CS. This practice gives information concerning the surface morphology of samples. PAA has a considerable number of hexagonal shaped pores, therefore there is a good probability for CS to adherent to the underlying alumina. Upon interaction of CS-PAA with Ag solution, the polar hydroxyl groups of CS bound the electropositive transition metal ions probably via electrostatic (i.e., ion–dipole) forces and reduce Ag^+ to Ag^0 [73]. Ag nano-structures were formed by reduction of Ag^+ with chitosan. SEM images (Fig. 2(b, c)) reflect a zigzag pattern of Ag nano-flakes created in CS web associated with hexagonal cells of PAA.

The existence of 93.71 (by weight %) Ag in nano-particles was also acknowledged by EDX analysis (Fig. 3).

XRD pattern draws four reflection peaks analogous to crystalline Ag peaks. Miller indices were assigned to each peak. These four peaks were allotted to diffraction from $2\theta = 38.01°$ (111), 44.28° (200), 64.46° (220) and 77.47° (311) of the Ag planes, correspondingly. The XRD peaks suggested face centered cubic phase for crystalline Ag with highly intense peak observed at index value of (111). Reflection peaks of CS biopolymer compatible to $2\theta = 53.02°$, 40.49°, 27.78°, 20.33° and 18.6° were also detected (Fig. 4). These peaks are fingerprint for CS crystallinity, principally an intense peak at ~20° [74].

Table 1: Experimental settings for fabrication of Ag and Au nano-structures on CS-PAA nano-composite along with their designations.

Sample Designation	Electro-polishing	1st Step Anodization [a]	2nd Step Anodization [b]	Bio-polymer-Porous anodic alumina nano-composite	Metal Deposition
CS/PAANS	20 V in C_2H_5OH-$HClO_4$ at 1°C for 20 min	50 V in 0.3M $C_2H_2O_4$ at 1°C for 3 h	50 V in 0.3M $C_2H_2O_4$ at 1°C for 3 h	Saturated CS solution in 5% CH_3COOH at room temperature for 24 h	1 mM precursor ($AgNO_3$ or $HAuCl_4.3H_2O$) solution for 24 h
γ-ICS/PAANS	20 V in C_2H_5OH-$HClO_4$ at 1°C for 20 min	50 V in 0.3M $C_2H_2O_4$ at 1°C for 3 h	50 V in 0.3M $C_2H_2O_4$ at 1°C for 3 h	Saturated γ-ICS solution in 5% CH_3COOH at room temperature for 24 h	1 mM precursor ($AgNO_3$ or $HAuCl_4.3H_2O$) solution for 24 h

a) Wet chemical etching of 1st step anodized layer in a mixture of 0.4 M H_3PO_4 and 0.2 M CrO_3.H_2O at 80 °C for 3h.

b) Pore widening in 0.3 M $C_2H_2O_4$ at room temperature for 30 min.

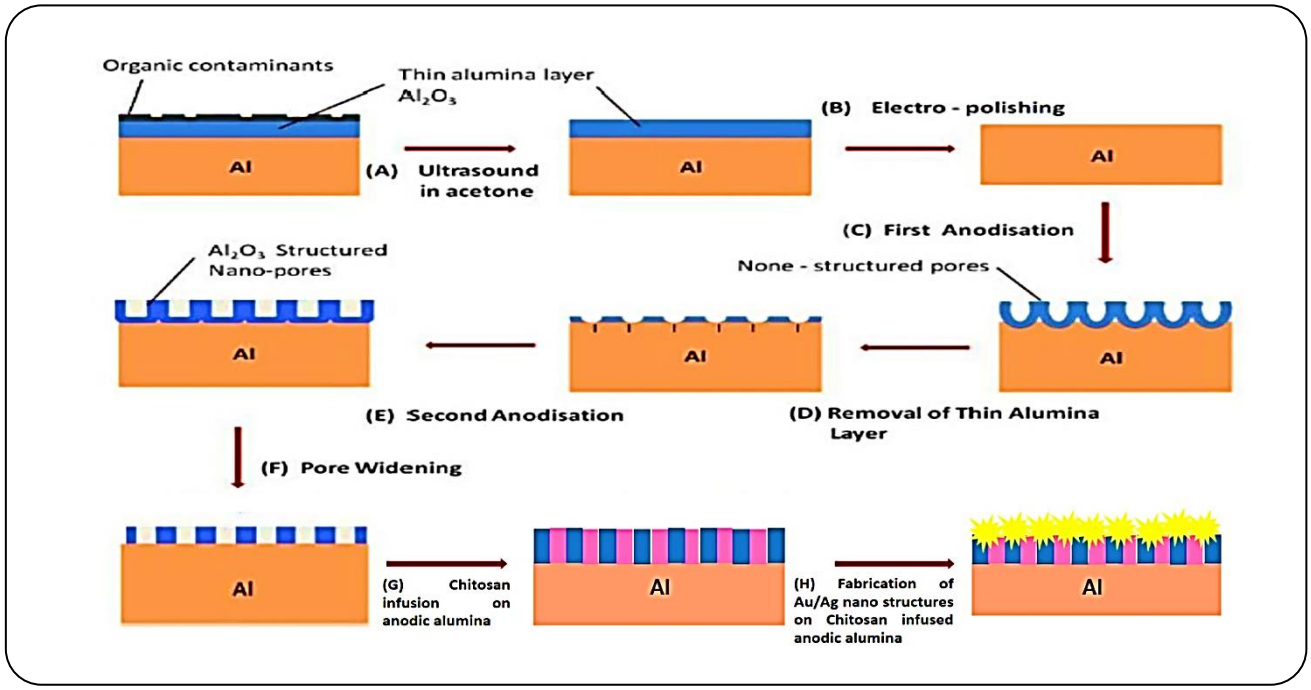

Fig. 1: Schematic diagram for metal nano-structure fabrication using CS/PAA nano-composite.

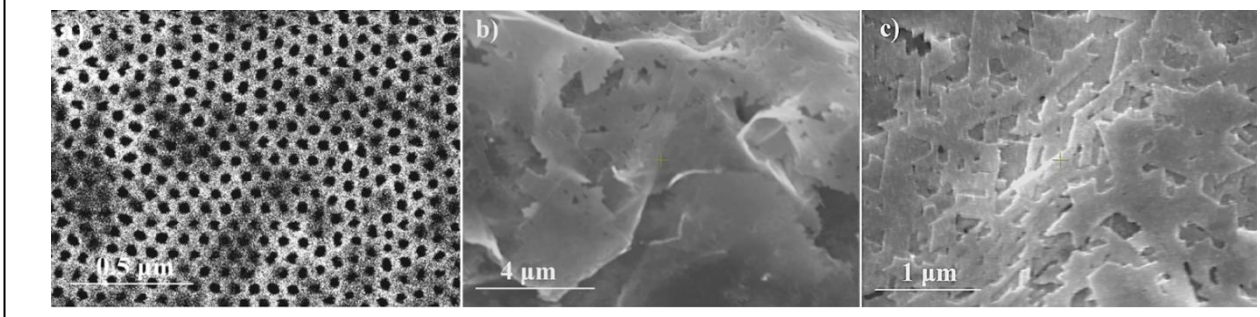

Fig. 2: (a) Di-step anodized aluminum strip showing a regular, closely organized hexagonal cells; (b, c) SEM micrograph of Ag-CS/PAANS showing formation of zigzag Ag nano-flakes.

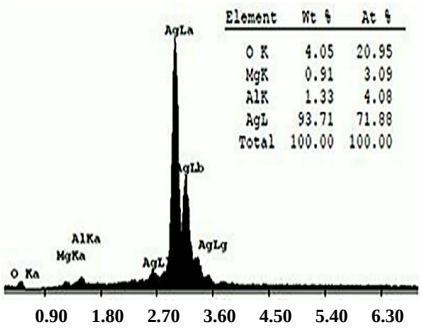

Fig. 3: EDX image of Ag-CS/PAANS.

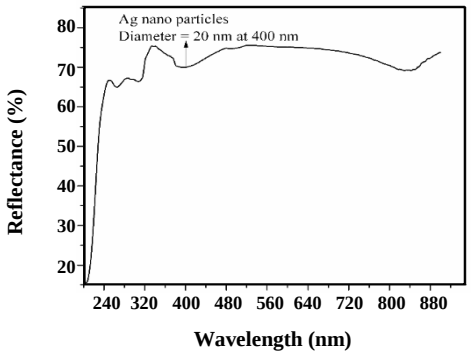

Fig. 5: Diffuse reflectance plot of Ag-CS/PAANS.

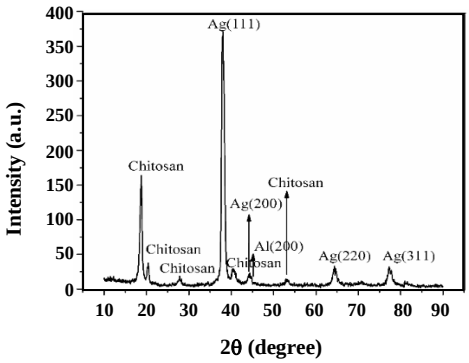

Fig. 4: XRD pattern of Ag-CS/PAANS.

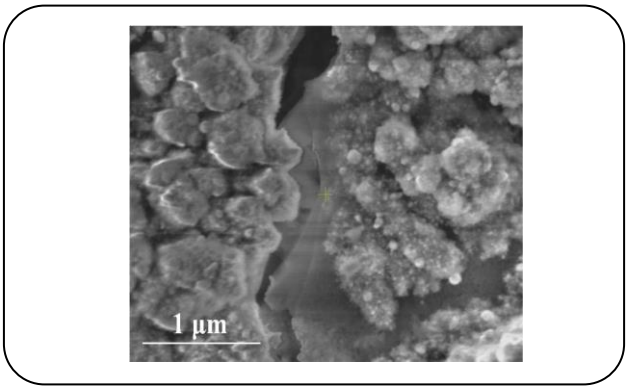

Fig. 6: SEM micrograph of Au-CS/PAANS clearly showing Au NS deposition.

PAA is transparent towards UV-Vis spectroscopy. The UV-Vis diffused reflectance spectrum of Ag-CS-PAA nano-composites shows a sole, strong minimum just about 400 nm (Fig. 5). This groove corresponds to the characteristic Surface Plasmon Resonance (SPR) of the valence electrons of Ag nano-structures. Silver nanoparticles show a typical Plasmon band at around 400–420 nm [73]. The estimated particle size from the position of the reflectance minima is 20 nm [77, 78].

Gold-chitosan/porous anodic alumina nano-structures (Au-CS/PAANS)

SEM image (Fig. 6) shows Au NS deposited on the CS-PAA nano-composite as almost spherical nano-particles. The various phenomenon for the uptake of gold metal ions by CS include adsorption, chelation and ion exchange. The amino groups of CS interacts with the metal ions either through chelation by utilizing the two amino groups from two glucosamine residues of the CS polymer chain, or through adsorption phenomena by active participation of its lone pair of electrons [76].

The EDX spectroscopy of the sample ratified the existence of Au NS. The weight percentage of Au was 29.06% as given in Fig. 7. Oxygen and aluminum peaks in EDX plot indicate the presence of Al_2O_3 of PAA.

In XRD pattern, the Brag reflections with 2θ values of 53º, 40.7º, 27.8º, 20.2º and 18.7º were recognized for the CS biopolymer [74, 75]. Reflection peaks corresponding to (111), (200), (220), (311) and (222) lattices were attributed towards face centered cubic Au. Preferential orientation of Au was along the (111) plane (Fig. 8). Aluminum reflection peaks (face centered cubic) corresponding to (200), (220) and (311) faces were also found.

The diffuse reflectance analysis (Fig. 9) of Au-CS/PAANS displayed a reflection minimum at 515 nm in the absorption series of Au nano-particles. The observed minimum corresponds to the typical SPR of valence shell electrons of Au nano-particles. Gold nanoparticles show a characteristic Plasmon band at ~520 nm and predicted size of 5 nm [73, 78, 79].

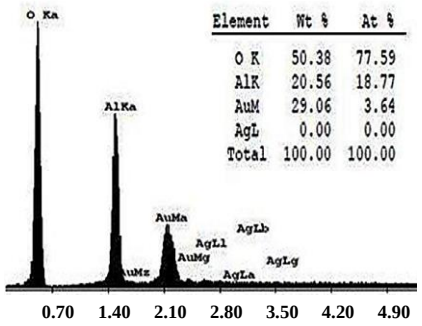

Fig. 7: EDX analysis of Au-CS/PAANS.

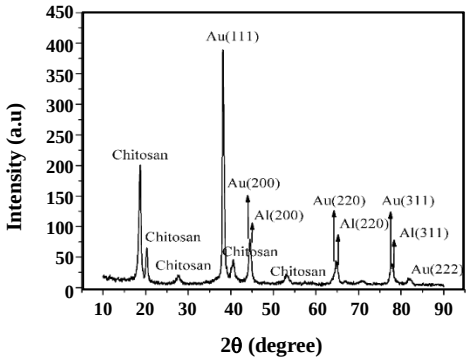

Fig. 8: XRD pattern of Au-CS/PAANS.

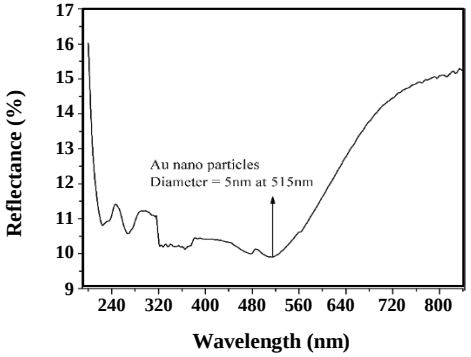

Fig. 9: Diffuse reflectance spectrum of Au-CS/PAANS.

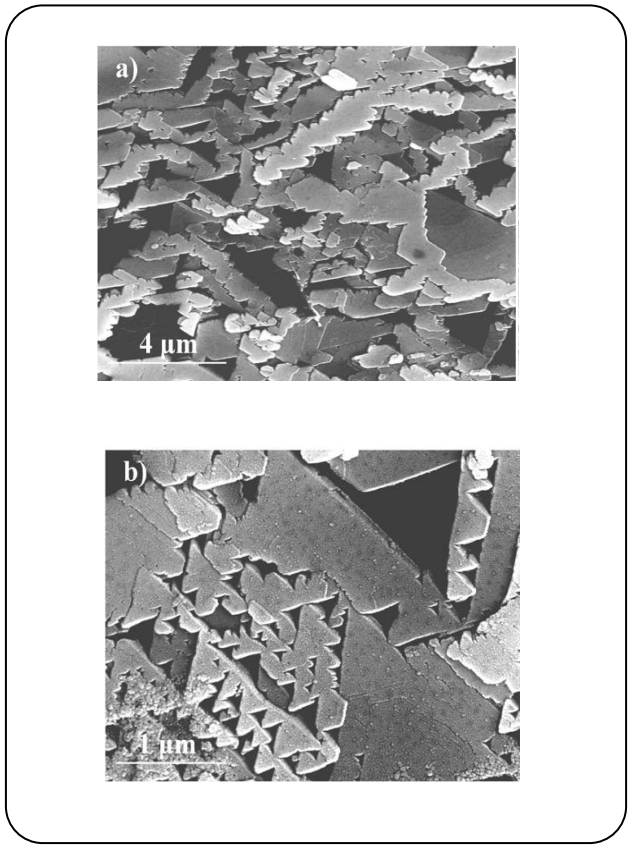

Fig. 10(a, b): SEM image of Ag-γ-ICS/PAANS showing that Ag deposited as nano-banners.

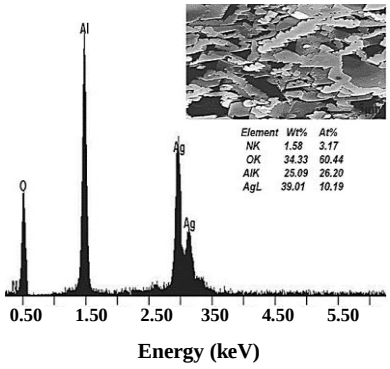

Fig.11: EDX plot of Ag-γ-ICS/PAANS nano-banners.

Silver-γ-irradiated chitosan/ porous anodic alumina nano-structures (Ag-γ-ICS/PAANS)

The length of chitosan biopolymer chains was minimized by irradiation with γ-rays. This enhances the association of chitosan chains to the PAA nano-hexagonal pore array. The widespread web of template hydrogen bonds prevents the aggregation of nanoparticles. γ-ICS stabilized the Ag^+ ions as nano-banners of triangular shape. These silver nano-banners are interlinked with each other and grow along the faces of the triangle. SEM images (Fig. 10a, b) clearly show these triangular chains.

EDX plot (Fig. 11) also confirmed that these triangular chains belong to Ag. These nano-banners consist of 39.01 weight % of Ag. Al and O peaks of PAA were also observed in EDX plot.

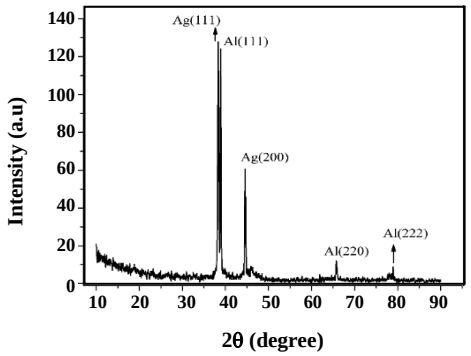

Fig. 12: XRD pattern of Ag-γ-ICS/PAANS.

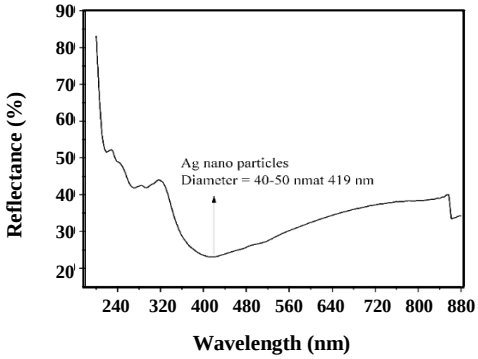

Fig. 13: Diffuse reflectance spectrum of Ag-γ-ICS/PAANS.

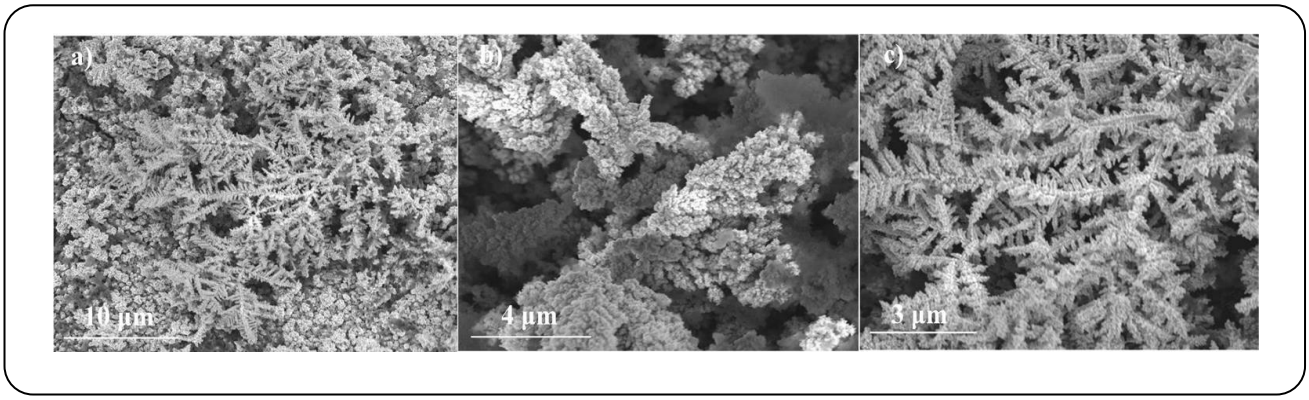

Fig. 14: (a) SEM micrograph of Au-γ-ICS/PAANS showing diverse morphologies for Au NS; (b) dendritic structures; (c) a network of pine leaves.

In XRD pattern, two reflection peaks corresponding to crystalline Ag were noticed. These peaks appeared at 2θ = 38.01°, 44.28° and indexed to (111), (200) planes. The reported reflections are in good agreement with standard values of the face centered cubic metallic Ag (Fig. 12). Reflections equivalent to (111), (220) and (222) Al planes were also found, suggesting a face centered cubic phase for crystalline Al. The observed high intensity peak for Ag as well as Al has an indexed value of (111).

In UV-Vis diffused reflectance spectrum of Ag-γ-ICS/PAA nano-composites, a single strong groove around 419 nm was observed (Fig. 13). This groove subscribes to valence electron SPR of the Ag nano-structures. 400-420nm is the typical Plasmon band range for silver nanoparticles [73]. From the position of the reflectance minima, the predictable particle size ranges from 40-50 nm [77, 78].

Associations of γ-ICS chains with PAA nano-hexagonal pores provides efficient stabilization to noble metal nano-particles via hydrogen bonding. SEM micrograph (Fig. 14a) reveals that γ-ICS stabilized Au in two attractive patterns i.e. dendritic structure and branched structure resembling the leaves of a pine tree. These fascinating patterns are evident in high magnification images (Fig. 14b, c). The observed branched structures may due to the nucleation effect of Au nano-particles [73].

Similarly, EDX map witnessed the belonging of these interesting patterns to Au (Fig. 15). The nano-pine leaves comprised of 75.90 (by weight percent) of Au.

Face centered cubic Al corresponding to the (111), (200), (220) and (311) planes were detected in X-ray diffraction spectrum. Al was preferably oriented along (111) Miller index. Sharp peaks corresponding to (111), (200), (220), (311) and (222) phases were also observed. These sharp peaks are indexed to highly crystalline, face centered cubic Au with special alignment along the (111) plane (Fig. 16).

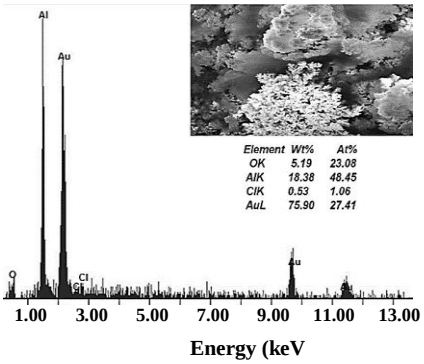

Fig. 15: EDX plot of Au-γ-ICS/PAANS.

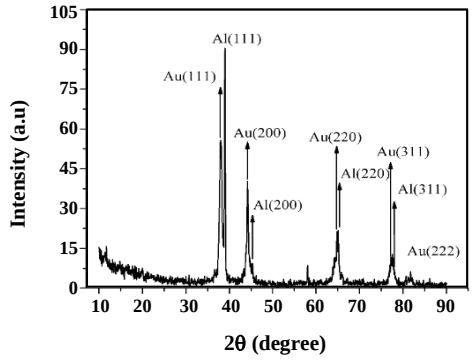

Fig. 16: XRD plot of Au-γ-ICS/PAAANS.

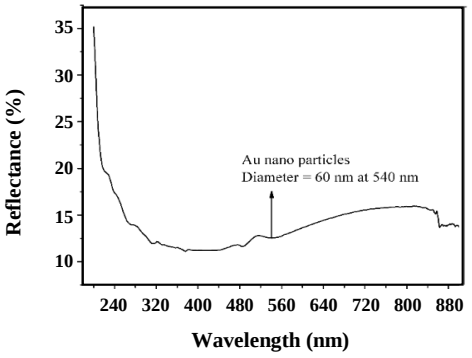

Fig. 17: Diffuse reflectance spectrum of Au-γ-ICS/PAANS.

The diffused reflection analysis of Au-γ-ICS/PAAANS gave a reflection minimum centered at 540 nm. This groove evidenced the formation of gold nano-particles on porous anodic alumina modified with γ-irradiated chitosan as shown in Fig. 17. Typically gold nano-particles show SPR at about 520nm. The observed Plasmon value may be due to unique dendritic and nano-pine leave arrangements [73]. Reflectance groove estimated gold nano-structure size is 60nm [78, 79].

The band gap energies for observed metal nano-structures can be calculated from their respective SPR wavelengths. These energies are given in Table 2.

CONCLUSIONS

- A simple, convenient, non-hazardous and reproducible procedure has been proposed for the preparation of Ag and Au NS using CS-PAA nano-composite. It was demonstrated that the combined stabilization and reduction effect of CS-PAA nano-composite is worth considering.
- PAA acted as guider and causes the alignment of polymer chains within the uniformly size pore array. The nano-porous nature of anodic alumina has also provided with regular anchoring points that are responsible for stability of the metal-polymer nano-composite film of the substrate.
- In case of γ-ICS, the gamma radiations lowered the molecular weight and crystallinity of CS by breaking the polymer backbone (dissociating the C–H and C–OH bonds of CS).
- CS and γ-ICS solutions uniformly associate with hex nano-pores of PAA and furnish many active sites for nucleation and crystal growth.
- During metal deposition, the amine functionality of CS will function as reducing agents for the formation of Au NS whereas electron rich oxygen atoms of hydroxyl groups of CS interact and reduce Ag^{+} to Ag^{0}.
- Both, γ-ICS and non-irradiated CS furnished interesting morphologies for Ag and Au NS which include Ag nano-banners, Au nano-pine leaves, Au dendritic structures, zigzag silver nano-flakes and a spherical Au nano-particles respectively.
- XRD crystalline diffraction peaks demonstrated face centered cubic phases for Ag and Au NS.
- Reflection minima in the absorption ranges of Ag and Au NS strengthened the presence of Ag and Au NS upon the respective samples.
- Furthermore, the EDX data also insisted the existence of Ag and Au NS.
- This prospective method can be engaged for the mass fabrication of Ag or Au-CS/PAANS which may serve the medical industry and also help in metal removal as it is environmentally benign.

Table 2: Surface Plasmon Resonance (SPR) wavelengths, particle sizes and band gap energies of observed metal nano-structures along with their designations [77-81].

Sample Designation	SPR Wavelength (m) x 10^7	Size (nm)	Band Gap Energy (eV)
Ag-CS/PAANS	4.00	20	3.10
Au-CS/PAANS	5.15	5	2.41
Ag-γ-ICS/PAANS	4.19	40-50	2.96
Au-γ-ICS/PAANS	5.40	60	2.30

Acknowledgements

The authors are pleased to acknowledge Professor Dr. Mazhar Mehmood, Department of Metallurgy and Materials Engineering (DMME), Pakistan Institute of Engineering and Applied Sciences (PIEAS), Islamabad, Pakistan, for granting permission to use lab facilities for the completion of this research work.

Received : May 5, 2018 ; Accepted : Sep. 15, 2018

REFERENCES

[1] Masuda H., Matsui Y., Yotsuya M., Matsumoto F., Nishio K., Fabrication of Highly Ordered Anodic Porous Alumina Using Self-organized Polystyrene Particle Array, *Chem. Lett.*, **33**(5): 584-585 (2004).

[2] Lee J., Nigo S., Nakano Y., Kato S., Kitazawa H., Kido G., Structural Analysis of Anodic Porous Alumina Used for Resistive Random Access Memory, *Sci. Technol. Adv. Mater.*, **11**(2): 025002-025006 (2010).

[3] Rauf A., Mehmood M., Rasheed M.A., Aslam M., The Effects of Electro-polishing on the Nano-channel Ordering of the Porous Anodic Alumina Prepared in Oxalic Acid. *J. Solid State Electr.*, **13**(2): 321-332 (2009).

[4] Sulka G.D., Brzozka A., Zaraska L., Jaskula M., Through-hole Membranes of Nano-porous Alumina Formed by Anodizing in Oxalic Acid and their Applications in Fabrication of Nanowire Arrays. *Electrochim. Acta.*, **55**(14): 4368-4376 (2010).

[5] Mutalib A., Losic D., Voelcker N.H., Nano-porous Anodic Aluminum Oxide: Advances in Surface Engineering and Emerging Applications, *Prog. Mater. Sci.*, **58**(5): 636-704 (2013).

[6] Santos A., Kumeria T., Losic D., Nano-porous Anodic Alumina: A Versatile Platform for Optical Biosensors, *Materials*, **7**(6): 4297-4320 (2014).

[7] Borrull J.F., Pallares J., Macias G., Marsal L.F., Nanostructural Engineering of Nanoporous Anodic Alumina for Biosensing Applications, *Materials*, **7**(7): 225-5253 (2014).

[8] Sriram G., Patil P., Bhat M.P., Hegde R.M., Ajeya K.V., Udachyan I., Bhavya M.B., Gatti M.G., Uthappa U.T., Neelgund G.M., Jung H.Y., Current Trends in Nanoporous Anodized Alumina Platforms for Biosensing Applications, *J. Nanomater.*, **2016**(2): 2-26 (2016).

[9] Yanagishita T., Kato A., Masuda H., Preparation of Ideally Ordered Through-hole Anodic Porous Alumina Membranes by Two-layer Anodization, *Jpn. J. Appl. Phys.*, **56**(3): 035202-035204 (2017).

[10] Chatterjee S., Sarkar J., Mallick A.B., Roy D., Deb P., Effect of Anodizing Medium on the Morphology and Photoluminescent Property of Porous Alumina Film, *J. Eng. Tech.*, **4**(2): 59-62 (2017).

[11] Roslyakov I.V., Elena O.G., Kirill S.N., Role of Electrode Reaction Kinetics in Self-ordering of Porous Anodic Alumina, *Electrochim. Acta.*, **241**: 362-369 (2017).

[12] Mezni A., Altalhi T., Saber N.B., Aldalbahi A., Boulehmi S., Santos A., Losic D., Size and Shape-Controlled Synthesis of Well-organised Carbon Nanotubes Using Nanoporous Anodic Alumina with Different Pore Diameters, *J. Colloid Interf. Sci.*, **491**: 375-389 (2017).

[13] Zhang Q., Li Y., Xu D., Gu Z., Preparation of Silver Nanowire Arrays in Anodic Aluminum Oxide Templates, *J. Mater. Sci. Lett.*, **20**(10): 925-927 (2001).

[14] Nielsch K., Muller F., Li A.P., Gosele U., Uniform Nickel Deposition into Ordered Alumina Pores by Pulsed Electrodeposition, *Adv. Mater.*, **12**(8): 582-586 (2000).

[15] Krolla M., Blaua W.J., Grandjeanb D., Benfieldb R.E., Luisc F., Paulusc P.M., De-Jongh L.J., Magnetic Properties of Ferromagnetic Nanowires Embedded in Nanoporous Alumina Membranes, *J. Magn. Magn. Mater.*, **249**(1-2): 241-245 (2002).

[16] Xu C.L., Li H., Zhao G.Y., Li H.L., Electrodeposition of Ferromagnetic Nanowire Arrays on AAO/Ti/Si Substrate for Ultrahigh-density Magnetic Storage Devices, *Mater. Lett.*, **60**(19): 2335-2338 (2006).

[17] Huczko A., Template-Based Synthesis of Nanomaterials, *Appl. Phys. A.*, **70**(4): 365-376 (2000).

[18] Shi W., Shen Y., Ge D., Xue M., Cao H., Huang S., Wang J., Zhang G., Zhang F., Functionalized Anodic Aluminum Oxide (AAO) Membranes for Affinity Protein Separation, *J. Membrane Sci.*, **325**(2): 801-808 (2008).

[19] Ding Y., Zhang P., Qub Y., Jiang Y., Huang J., Yan W., Liu G., AFM Characterization and Electrochemical Property of Ag Nanowires by Modified AAO Template Method, *J. Alloy Compd.*, **466**(1-2): 479-482 (2008).

[20] Hanaoka T.A., Heilmann A., Kroll M., Kormann H.P., Sawitowski T., Schmid G., Jutzi P., Klipp A., Kreibig U., Neuendorf R., Alumina Membranes—Templates for Novel Nanocomposites, *Appl. Organomet. Chem.*, **12**(5): 367-373 (1998).

[21] Noyan A.A., Leontiev A.P., Yakovlev M.V., Roslyakov I.V., Tsirlina G.A., Napolskii K.S., Electrochemical Growth of Nanowires in Anodic Alumina Templates: The Role of Pore Branching, *Electrochim. Acta.*, **226**(1): 60-68 (2017).

[22] Chik H., Xu J., Nanometric Superlattices: Non-lithographic Fabrication, Materials, and Prospects, *Mater. Sci. Eng., R.*, **43**(4): 103-138 (2004).

[23] Shingubara S., Okino O., Murakami Y., Sakaue H., Takahaqi T., Fabrication of Nanohole Array on Si Using Self-organized Porous Alumina Mask, *J. Vac. Sci. Technol. B.*, **19**(5): 1901-1904 (2001).

[24] Thorat S., Diaspro A., Scarpellini A., Povia M., Salerno M., Comparative Study of Loading of Anodic Porous Alumina with Silver Nanoparticles Using Different Methods, *Mater.*, **6**(1): 206-216 (2013).

[25] Forrer P., Schlottig F., Siegenthaler H., Textor M., Electrochemical Preparation and Surface Properties of Gold Nanowire Arrays Formed by the Template Technique, *J. Appl. Electrochem.*, **30**(5): 533-541 (2000).

[26] Sulka G.D., Brzozka A., Liu L., Fabrication of Diameter-Modulated and Ultrathin Porous Nanowires in Anodic Aluminum Oxide Templates, *Electrochim. Acta.*, **56**(14): 4972-4979 (2011).

[27] Park H., Kim T.H., Kang S.W., Jeong S.H., Nanoscale Reaction Vessels: Highly Ordered Nanocrystal Arrays Inside Porous Anodic Alumina Nanowells, *Int. J. Electrochem. Sci.*, **10**(10): 8447 – 8453 (2015).

[28] Choi J., Sauer G., Nielsch K., Wehrspohn R.B., Gosele U., Hexagonally Arranged Monodisperse Silver Nano-wires with Adjustable Diameter and High Aspect Ratio, *Chem. Mater.*, **15**(3): 776-779 (2003).

[29] Yang R., Sui C., Gong J., Qu L., Silver Nanowires Prepared by Modified AAO Template Method, *Mater. Lett.*, **61**(3): 900-903(2007).

[30] Narayan R.J., Aggarwal R., Wei W., Jin C., Monteiro-Riviere N.A., Crombez R., Mechanical and Biological Properties of Nanoporous Carbon Membranes, *Biomed. Mater.*, **3**(3): 034107 (2008).

[31] Lee S.B., Mitchell D.T., Trofin L., Nevanen T.K., Soderlund H., Martin C.R., Antibody-Based Bionanotube Membranes for Enantiomeric Drug Separations, *Sci.*, **296**(5576): 2198-2200 (2002).

[32] Winkler B., Modification of the Surface Characteristics of Anodic Alumina Membranes Using Sol–gel Precursor Chemistry, *J. Membrane Sci.*, **226**(1-2):75-84 (2003).

[33] Skoog S.A., Bayati M.R., Petrochenko P.E., Stafslien S., Daniels J., Cilz N., Antibacterial Activity of Zinc Oxide Coated Nanoporous Alumina, *Mater. Sci. Eng. B.*, **177**(12): 992-998 (2012).

[34] Kovtyukhova N.I., Mallouk T.E., Mayer T.S., Templated Surface Sol-gel Synthesis of SiO_2 Nanotubes and SiO_2 Insulated Metal Nanowires, *Adv. Mater.*, **15**(10): 780-785 (2003).

[35] Cameron M.A., Gartland I.P., Smith J.A., Diaz S.F., George S.M., Atomic Layer Deposition of SiO_2 and TiO_2 in Alumina Tubular Membranes: Pore Reduction and Effect of Surface Species on Gas Transport, *Langmuir*, **16**(19): 7435-7444 (2000).

[36] Vajandar S.K., Xu D., Markov D.A., Wikswo J.P., Hofmeister W., Li D., SiO_2 Coated Porous Anodic Alumina Membranes for High Flow Rate Electroosmotic Pumping, *Nanotechnology*, **18**(27): 275705 (2007).

[37] Matsumoto F., Nishio K., Masuda H., Flow-through-type DNA Array Based on Ideally Ordered Anodic Porous Alumina Substrate, *Adv. Mater.*, **16**(23-24): 2105-2108 (2007).

[38] Milka P., Krest I., Keusgen M., Immobilization of Alliinase on Porous Aluminum Oxide, *Biotechnol. Bioeng.*, **69**(3): 344-348 (2000).

[39] ter Maat J., Regeling R., Ingham C.J., Weijers C.A., Giesbers M., de Vos W.M., Zuilhof H.. Organic Modification and Subsequent Biofunctionalization of Porous Anodic Alumina Using Terminal Alkynes. *Langmuir*, **27**(22): 13606-13617 (2011).

[40] Aramesh M., Fox K., Lau D.W.M., Fang J.H., Ostrikov K., Prawer S., Cervenka J., Multifunctional Three Dimensional Nanodiamond Nanoporous Alumina Nanoarchitectures, *Carbon*, **75**: 452- 464 (2014).

[41] Skoog S.A., Sumant A.V., Monteiro-Riviere N.A., Narayan R.J., Ultrananocrystalline Diamond-Coated Microporous Silicon Nitride Membranes for Medical Implant Applications, *JOM*, **64**(4): 520-525 (2012).

[42] Karan S., Samitsu S., Peng X., Kurashima K., Ichinose I., Ultrafast Viscous Permeation of Organic Solvents Through Diamond Like Carbon Nanosheets, *Sci.*, **335**(6067): 444-447 (2012).

[43] Popat K.C., Mor G., Grimes C.A., Desai T.A., Surface Modification of Nanoporous Alumina Surfaces with Poly(ethylene glycol), *Langmuir*, **20**(19): 8035-8041 (2004).

[44] Lee S.W., Shang H., Haasch R.T., Petrova V., Lee G.U., Transport and Functional Behaviour of Poly(ethylene glycol) Modified Nanoporous Alumina Membranes, *Nanotechnology*, **16**(8): 1335-1340 (2005).

[45] Simovic S., Losic D., Vasilev K., Controlled Drug Release from Porous Materials by Plasma Polymer Deposition, *Chem. Commun.*, **46**(8): 1317-1319 (2010).

[46] Aw M.S., Simovic S., Addai-Mensah J., Losic D., Polymeric Micelles in Porous and Nanotubular Implants as a New System for Extended Delivery of Poorly Soluble Drugs, *J. Mater. Chem.*, **21**(20): 7082-7089 (2011).

[47] Bruening M.L., Dotzauer D.M., Jain P., Ouyang L., Baker G.L., Creation of Functional Membranes Using Polyelectrolyte Multilayers and Polymer Brushes, *Langmuir*, **24**(15): 7663-7673 (2008).

[48] Nagale M., Kim B.Y., Bruening M.L., Ultrathin, Hyperbranched Poly(Acrylic Acid) Membranes on Porous Alumina Supports, *J. Am. Chem. Soc.*, **122**(47): 11670-11678 (2000).

[49] Pearce M.E., Jessica B., Melanko, Salem A.K., Multifunctional Nanorods for Biomedical Applications, *Pharm. Res.*, **24**(12): 2335-2352 (2007).

[50] Wei J., Xue D., Xu Y., Photoabsorption Characterization and Magnetic Property of Multiferroic $BiFeO_3$ Nanotubes Synthesized by a Facile Sol–gel Template Process, *Scripta Mater.*, **58**(1): 45-48 (2008).

[51] Naghizadeh A., Ghafouri M., Synthesis and Performance Evaluation of Chitosan Prepared from Persian Gulf Shrimp Shell in Removal of Reactive Blue 29 Dye from Aqueous Solution (Isotherm, Thermodynamic and Kinetic Study). *Iran. J. Chem. Chem. Eng. (IJCCE), 36*(3): 25-36 (2017).

[52] Kumar M.N.V.R., A Review of Chitin and Chitosan Applications, *React. Funct. Polym.*, **46**(1): 1-27 (2000).

[53] Lee M., Chen B.Y., Den W., Chitosan as a Natural Polymer for Heterogeneous Catalysts Support: A Short Review on its Applications, *Appl. Sci.*, **5**(4): 1272-1283 (2015).

[54] Austin P.R., Brine C.J., Castle J.E., Zikakis J.P., Chitin: New facets of research. *Sci.*, **212**(4496): 749-753 (1981).

[55] Raoufi M., Aslankoohi N., Mollenhauer C., Boehm H., Spatz J.P., Bruggemann D., Template-Assisted Extrusion of Biopolymer Nanofibers Under Physiological Conditions, *Integr. Biol-UK*, **8**: 1059-1066 (2016).

[56] Berger J., Reist M., Mayer J.M., Felt O., Gurny R., Structure and Interactions in Chitosan Hydrogels Formed by Complexation or Aggregation for Biomedical Applications, *Eur. J. Pharm. Biopharm.*, **57** (1): 35-52 (2004).

[57] Mohanasrinivasan V., Mishra M., Paliwal J.S., Singh S.K., Selvarajan E., Suganthi V., Devi C.S., Studies on Heavy Metal Removal Efficiency and Antibacterial Activity of Chitosan Prepared from Shrimp Shell Waste, 3 *Biotech*., **4**(2): 167-175 (2014).

[58] Huang H., Yuan Q., Yang X., Morphology Study of Gold–Chitosan Nanocomposites, *J. Colloid Interf. Sci*., **282**(1): 26-31(2005).

[59] Wang M., Qiang J., Fang Y., Hu D., Cui Y., Fu X., Preparation and Properties of Chitosan-Poly (N-isopropylacrylamide) Semi-IPN Hydrogels, *J. Polym. Sci. Pol. Chem.*, **38**(3): 474-481 (2000).

[60] Wang B., Chen K., Jiang S., Reincke F.O., Tong W., Wang D., Gao C., Chitosan-Mediated Synthesis of Gold Nanoparticles on Patterned Poly (dimethylsiloxane) Surfaces, *Biomacromolecules*., **7**(4): 1203-1209 (2006).

[61] Sun L., Yuan Z., Gong W., Zhang L., Xu Z., Su G., Han D., The Mechanism Study of Trace Cr (VI) Removal from Water Using Fe 0 Nanorods Modified with Chitosan in Porous Anodic Alumina, *Appl. Surf. Sci.*, **328**(15): 606-613 (2015).

[62] Shi W., Shen Y., Ge D., Xue M., Cao H., Huang S., Wang J., Zhang G., Zhang F., Functionalized Anodic Aluminum Oxide (AAO) Membranes for Affinity Protein Separation, *J. Membrane Sci*., **325**(2): 801-808 (2008).

[63] Mehmood M., Rauf A., Rasheed M.A, Saeed S., Akhter J.I., Ahmad J., Aslam M., Preparation of Transparent Anodic Alumina with Ordered Nanochannels by Through-thickness Anodic Oxidation of Aluminum Sheet, *Mater. Chem. Phys.*, **104**(2-3): 306-311 (2007).

[64] Huang Y., Yu H., Guo L., Huang Q., Structure and Self-Assembly Properties of a New Chitosan-Based Amphiphile, *J. Phys. Chem. B*., **114**(23): 7719-7726 (2010).

[65] Tahtat D., Uzun C., Mahlous M., Güven O., Beneficial Effect of Gamma Irradiation on the N-Deacetylation of Chitin to Form Chitosan, *Nucl. Instrum. Methods Phys. Res., Sect. B*, **265**(1): 425-428 (2007).

[66] Zainol I., Akil H.M., Mastor A., Effect of γ-irradiation on the Physical and Mechanical Properties of Chitosan Powder, *Mater. Sci. Eng., C*, 29(1): 292-297 (2009).

[67] Baroudi A., García-Payo C., Khayet M., Structural, Mechanical, and Transport Properties of Electron Beam-irradiated Chitosan Membranes at Different Doses, *Polymers*, **10**(2): 117-140 (2018).

[68] Nho Y.C., Park S.E., Kim H.I., Hwang T.S., Retracted: Oral Delivery of Insulin Using pH-Sensitive Hydrogels Based on Polyvinyl Alcohol Grafted with Acrylic Acid/Methacrylic Acid by Radiation, *Nucl. Instrum. Methods Phys. Res., Sect. B*, **236**(1-4): 283-288 (2005).

[69] Islam A., Yasin T., Rehman I.U., Synthesis osf Hybrid Polymer Networks of Irradiated Chitosan/Poly (vinyl alcohol) for Biomedical Applications, *Radiat. Phys. Chem.*, **96**: 115- 119 (2014).

[70] Wasikiewicz J.M., Yoshii F., Nagasawa N., Wach R.A., Mitomo H., Degradation of Chitosan and Sodium Alginate by Gamma Radiation, Sonochemical and Ultraviolet Methods, *Radiat. Phys. Chem.*, **73**(5): 287-295 (2005).

[71] Dubey K.A., Bhardwaj Y.K., Chaudhari C.V., Kumar V., Goel N.K., Sabharwal S., Radiation Processed Ethylene Vinyl Acetate-Multiple Walled Carbon Nanotube Nano-Composites: Effect of MWNT Addition on the Gel Content and Crosslinking Density, *Express Polym. Lett*., **3**(8): 492-500 (2009).

[72] Lundvall O., Gulppi M., Paez M.A., Gonzalez E., Zagal J.H., Pavez J., Thompson G. E., Copper Modified Chitosan for Protection of AA-2024, *Surf. Coat. Tech.*, **201**(12): 5973-5978 (2007).

[73] Huang H., Yuan Q., Yang X., Preparation and Characterization of Metal–chitosan Nanocomposites, *Colloids Surfaces B.*, **39**(1-2): 31-37 (2004).

[74] Kumirska J., Czerwicka M., Kaczyński Z., Bychowska A., Brzozowski K., Thöming J., Stepnowski P., Application of Spectroscopic Methods for Structural Analysis of Chitin and Chitosan, *Mar. Drugs*, **8**(5): 1567-1636 (2010).

[75] Zhang Y., Xue C., Xue Y., Gao R., Zhang X., Determination of the Degree of Deacetylation of Chitin and Chitosan by X-ray Powder Diffraction, *Carbohyd. Res.*, **340**(11): 1914-1917 (2005).

[76] Ngah, W.S.W., Teong L.C., Hanafiah M.A.K.M., Adsorption of Dyes and Heavy Metal Ions by Chitosan Composites: A Review, *Carbohyd. Polym.*, **83**(4): 1446-1456 (2011).

[77] Paramelle D., Sadovoy A., Gorelik S., Free P., Hobley J., Fernig D.G., A Rapid Method to Estimate the Concentration of Citrate Capped Silver Nanoparticles from UV-Visible Light Spectra, *Analyst*, **139**(19): 4855-4861 (2014).

[78] Zuber A., Purdey M., Schartner E., Forbes C., Hoek B.V.D., Giles D., Abell A., Monro T., Heidepriem H.E., Detection of Gold Nanoparticles with Different Sizes Using Absorption and Fluorescence Based Method, *Sensor Actuat., B Chem.*, **227**: 117-127 (2016).

[79] Rahman S., Size and Concentration Analysis of Gold Nanoparticles with Ultraviolet-Visible Spectroscopy, *Undergraduate J. Math. Modeling: One + Two (UJMM)*, **7**(1): 2 (2016).

[80] Dharma J., Pisal A., Shelton C.T., Simple Method of Measuring the Band Gap Energy Value of TiO_2 in the Powder form using a UV/Vis/NIR Spectrometer, *Application Note*, (2009).

[81] Budhiraja N., Sharma A., Dahiya S., Parmar R., Vidyadharan V., Synthesis and Optical Characteristics of Silver Nanoparticles on Different Substrates, *Int. Lett. Chem. Phys. Astron.*, **14**: 80-88 (2013).